

Inverse Monte Carlo calculation of the effective pair interactions in FePd

This article has been downloaded from IOPscience. Please scroll down to see the full text article.

2005 J. Phys.: Condens. Matter 17 485

(<http://iopscience.iop.org/0953-8984/17/3/007>)

View [the table of contents for this issue](#), or go to the [journal homepage](#) for more

Download details:

IP Address: 129.252.86.83

The article was downloaded on 27/05/2010 at 19:46

Please note that [terms and conditions apply](#).

Inverse Monte Carlo calculation of the effective pair interactions in FePd

Tarik Mehaddene

Physik Department E13/FRMII, Technische Universität München, 85747 Garching, Germany

E-mail: mtarik@ph.tum.de

Received 25 October 2004, in final form 29 November 2004

Published 7 January 2005

Online at stacks.iop.org/JPhysCM/17/485

Abstract

Warren–Cowley short-range order parameters deduced from diffuse neutron scattering in an FePd single crystal have been used to calculate the effective pair interaction energies using an inverse Monte Carlo method. The pair interaction energies agree well with those obtained recently using an inverse cluster variation method and show a strong attraction between second-nearest-neighbour like atoms. The inverse Monte Carlo calculations show, in contrast to the direct cluster variation method, that the pair interactions in FePd are vanishing beyond the sixth atomic shell. The relevance of the calculated pair interactions is tested in terms of the order–disorder transition temperature simulation. A satisfactory agreement with the experimental value is observed.

1. Introduction

In substitutional solid solutions, the alloying atoms do not randomly occupy the lattice sites. Short-range order (SRO) is observed at higher temperature while below critical temperatures long-range order (LRO) or phase decomposition is seen. A precise knowledge of the SRO and of the atomic interactions responsible of it is therefore of basic interest for calculations of thermodynamic properties and phase diagrams [1–3]. Diffuse scattering of x-rays and neutrons remains the technique of choice for quantitative studies of the SRO. Over the last 50 years, the measurements have evolved significantly and, at present, they are carried out with a high degree of accuracy in single crystals at high and low temperature [4–11]. On the theoretical side, the study of SRO in alloys and its characterization through diffuse scattering has also been significantly improved since the pioneering work of Cowley [12], Krivoglaz [13] and Clapp and Moss [14] out of which emerged the well known Krivoglaz–Clapp–Moss formula (KCM). At present, several methods, aimed at extracting the pair interaction energies, providing a significant improvement over the KCM formula have been proposed. Among the approaches the most commonly used are the generalized perturbation method [15], in which the interactions are obtained by perturbation of the random alloy, and the real space inverse cluster variation

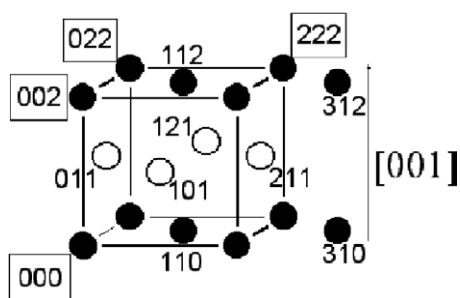


Figure 1. $L1_0$ -ordered phase with the different atomic occupations (\bullet Fe and \circ Pd). The labels give the shell index lmn . The positions always occupied by Fe are framed.

method (CVM) introduced by Gratias and C en ed ese [16]. Basically, the inverse CVM consists in minimizing a free energy functional where the entropy is a linear combination of entropies of finite clusters included in a given basic cluster. This method has been recently applied to extract the pair interaction energies in FePd using the Warren–Cowley SRO measured by *in situ* neutron diffuse scattering in an FePd single crystal at 1020 K [17]. While it is relatively straightforward to implement, the inverse CVM becomes computationally very intensive for large cluster approximations. Thus, the fitting is typically done for a relatively small number of SRO parameters. In fcc-based alloys, the commonly used approximation consists in using two maximum clusters, the face centred cube and the 13-point cubo-octahedron [18]. This cluster combination allows the calculation of only the first four and the sixth effective pair interactions and results in interactions that may be unrealistically short range for the alloy under investigation. To a great extent, this problem can be solved by an alternative approach, which consists in fitting the pair correlations by an inverse Monte Carlo method in real space [19], in which case longer interaction ranges may be included without any significant computational overhead.

In this paper, the inverse Monte Carlo method is applied to calculate the pair interaction energies in FePd using the same Warren–Cowley SRO parameters as deduced in [17]. Around the 50/50 stoichiometry, FePd orders in the $L1_0$ structure, made of alternating pure iron and pure palladium (001) planes (figure 1), and undergoes an order–disorder transition to the fcc-disordered state at 920 K [20]. The very anisotropic chemical order of the $L1_0$ structure is accompanied by a strong magnetic anisotropy and a tetragonality $c/a \approx 0.97$. The pronounced anisotropic properties of FePd are at the core of the present renewed interest in this system which is a good candidate for magneto-optical-storage devices [21, 22] and has potential applications as actuators and coupling devices [23]. Consequently, an additional motivation of the current work was to provide a detailed characterization of the chemical order and of the underlying interaction energies in a system with potentially important engineering applications.

2. Computational model

Lattice models have been widely and successfully used for computing the equilibrium thermodynamic properties of crystalline alloys. In a binary lattice model, the occupation of each site i in a lattice can be represented by a spin-like operator $\sigma_i = \pm 1$. The arrangement of atoms on the entire lattice is then given by $\sigma = \sigma_1, \sigma_2, \dots, \sigma_N$, where N is the number of sites in the lattice. In this representation, the total energy of the alloy can be written in terms of σ as a cluster expansion containing many-body contributions [15, 24]. Bieber and Gautier [25]

have shown that in transition metal alloys the predominant terms of the latter expansion are the pair interaction terms.

In order to calculate the pair interaction energies from the Warren–Cowley SRO parameters, we consider an Ising Hamiltonian which contains effective pair interactions:

$$H = \frac{1}{2} \sum_{i,j} V_{ij} \sigma_i \sigma_j \quad (1)$$

where σ_i is the occupation operator on site i . Its value is equal to 1 or -1 when the site is occupied by an Fe or Pd atom respectively. V_{ij} is the effective pair interaction between atoms at sites i and j and can be written as

$$V_{ij} = 1/4[v_{ij}^{\text{FeFe}} + v_{ij}^{\text{PdPd}} - 2v_{ij}^{\text{FePd}}]. \quad (2)$$

For convenience the various pair-interaction energies V_{ij} can be labelled by the shell index (lmn) or the shell number n . In principle, it is also possible to introduce a magnetic term in the Hamiltonian and to define effective pair interactions which have both chemical and magnetic contributions. However, in the Fe–Al system that is magnetically similar to Fe–Pd, Pierron-Bohnes *et al* have shown that the interplay between chemical and magnetic SRO is negligible above $T/T_{\text{Curie}} = 1.2$ [26, 27]. In FePd, $T_{\text{Curie}} = 760$ K. The measurement temperature (1020 K) [17] is thus high enough ($T/T_{\text{Curie}} = 1.34$) to neglect the magnetic interactions.

The pair interaction energies V_n are linked to the SRO parameters α_n by the Ising Hamiltonian (equation (1)). The SRO parameters are related to the correlation functions by

$$\alpha_n = \frac{\langle \sigma_0 \sigma_n \rangle - \langle \sigma_0 \rangle^2}{1 - \langle \sigma_0 \rangle^2} \quad (3)$$

where σ_0 and σ_n are the occupation operators at the origin and site n , respectively. The brackets stand for configurational averages.

The effective pair interaction energies are *a priori* unknown and will be discovered considering a three-dimensional lattice of L^3 fcc cells with cubic lattice constant a and linear periodic boundary conditions in all directions. Each site i of the lattice is occupied either by an Fe atom or a Pd atom. In accord with the stoichiometry of the $L1_0$ structure, there are as many Fe as Pd atoms. The modelling procedure starts with a random distribution. The evolution of the system is then simulated in the canonical ensemble i.e., based on exchanges of unlike atoms between different sites. A large number of exchanges between unlike atom pairs are attempted, each with a success ratio given by the Glauber algorithm: the exchange is performed if the Glauber probability

$$P(\Delta H) = \frac{\exp(-\Delta H/k_B T)}{1 + \exp(-\Delta H/k_B T)} \quad (4)$$

is larger than a random number between zero and unity. k_B and T are the Boltzmann constant and absolute temperature, respectively. ΔH is the energy balance of the exchange, evaluated using equation (1), where the sum runs over a given number of interacting atomic shells, considering the final and the initial configurations. We will refer to one Monte Carlo cycle as the number of Monte Carlo attempts necessary to visit every crystal site once on average. The SRO parameters are calculated for the considered number of interacting shells. At the same stage, the matrix A of the partial derivatives $\delta\alpha_n/\delta V_m$ is also calculated. A feedback process, that consists of comparing the calculated SRO parameters (α_n^{cal}) to the measured ones (α_n^{exp}) and rescaling the pair interaction energies accordingly, by solving the linear system $\Delta\alpha = A\Delta V$, is then executed every Monte Carlo cycle. $\Delta\alpha$ is the vector representing the difference between α_n^{cal} and α_n^{exp} and ΔV the corresponding difference in the amplitude of

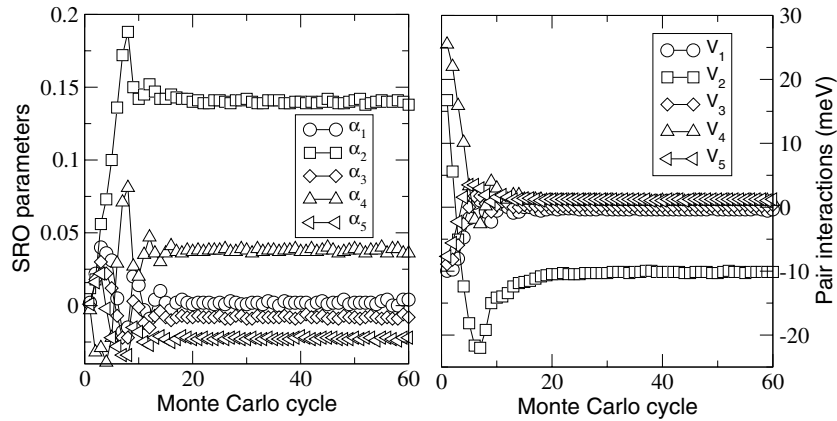


Figure 2. Evolution for the first five coordination shells of the Warren–Cowley SRO parameters (left) and the pair interaction energies (right) during the relaxation of the system toward the final equilibrium configuration obtained for $L = 50$ considering interactions up to the ninth nearest neighbours.

the pair interactions. The process is carried on until the system reaches the final equilibrium configuration in which the calculated SRO parameters are very close to the experimental ones. In this way, values of the effective pair interaction energies have been determined up to the ninth atomic shell. The calculations have been performed using the *Discus* package [28].

3. Results and discussion

To ensure that the linear dimensions of the simulation box are large enough compared to the correlation length of the SRO, calculations have been performed for different model crystals with linear dimension L varying from ten to 50 fcc cells with interacting shells from the fifth up to the ninth nearest neighbours. An example of the evolution of the pair interaction energies and the Warren–Cowley SRO parameters during the relaxation of the system toward the equilibrium configuration is shown in figure 2. The SRO parameters, as well as the pair interaction energies, become stable after approximately 25 Monte Carlo cycles. To ensure a final equilibrium state, calculations have been carried on up to 100 Monte Carlo cycles and statistical averages performed over the last 40 equilibrium configurations. The residual value $R = \sum_n |\alpha_n^{\text{cal}} - \alpha_n^{\text{exp}}| / \sum_n |\alpha_n^{\text{exp}}|$ of the experimental and the simulated SRO parameters has been calculated for different crystal dimensions considering the first nine coordination shells. The results are reported in figure 3. We see clearly that the quality of the fit is rather bad for small model crystals and gets better increasing the size of the simulation box. Its value is in the order of 10^{-4} for $L = 40$ and 50, in which cases only small deviations ($\simeq 1\text{--}2\%$) in the final pair interactions have been found. In order to reveal any correlation between the parameters, further calculations have been performed for the model crystal containing 50^3 fcc cells considering a decreasing number of atomic shells from the ninth up to fifth nearest neighbours. It turned out that the correlations between the parameters are rather small and the pair interaction energies deduced for different numbers of interacting shells are within the error bars. In fact, in the case of the pairwise interaction model, the correlations are usually small. Besides, the inverse Monte Carlo method would not produce reliable results if there were strong correlations between the parameters for instance, because of less appropriate choice of the interaction model or insufficient information about the SRO configuration.

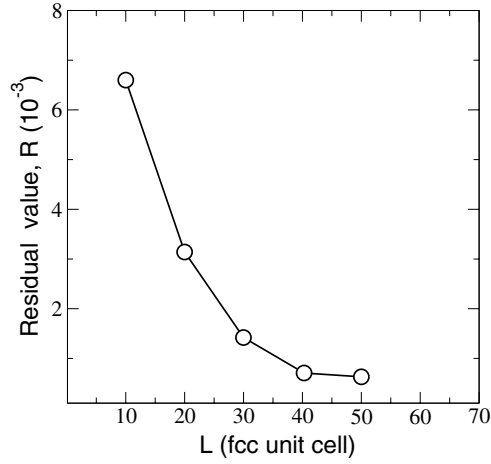


Figure 3. Residual value R versus the linear size of the model crystal calculated considering the first nine coordination shells.

Table 1. Experimental (α_n^{exp}) and calculated (α_n^{cal}) Warren–Cowley SRO parameters. Pair interaction energies (in meV) deduced from inverse Monte Carlo calculations (V_n^{IMC}). For comparison the results of the direct and inverse (underlined) CVM (V_n^{CVM}) [17] are also reported. The uncertainties ΔV_n^{CVM} and ΔV_n^{IMC} are estimated from the error bars on the experimental SRO parameters for V_n^{CVM} and from both experimental errors and the statistical averages for V_n^{IMC} .

Shell (n)	lmn	$2R_{lmn}/a$	$10^2\alpha_n^{\text{exp}}$	$10^2\alpha_n^{\text{cal}}$	V_n^{IMC}	ΔV_n^{IMC}	V_n^{CVM}	ΔV_n^{CVM}
1	110	1.141	0.19(37)	0.1899	-0.32	0.34	<u>-0.43</u>	0.33
2	200	2.000	13.99(56)	13.998	-10.31	1.1	<u>-11.76</u>	1.11
3	211	2.449	-0.79(22)	-0.795	0.22	0.3	<u>0.47</u>	0.20
4	220	2.828	3.79(30)	3.79	0.90	0.28	<u>0.85</u>	0.88
5	310	3.162	-2.25(23)	-2.252	1.19	0.31	1.97	0.20
6	222	3.464	2.95(30)	2.951	-1.14	0.4	<u>-1.54</u>	0.63
7	321	3.741	-1.27(16)	-1.27	0.35	0.36	1.11	0.14
8	400	4.000	2.44(45)	2.432	-0.18	0.28	-2.14	0.40
9	330	4.242	-0.30(27)	-0.298	0.14	0.28	0.26	0.23

The results of the calculations obtained for the model crystal with $L = 50$ considering interactions up to the ninth nearest neighbours are discussed, in the following, in terms of diffuse intensity profiles and pair interaction energies.

The diffuse intensity has been reconstructed in the (100) and (110) reciprocal planes from the final equilibrium values of the SRO parameters (α_n^{cal}) listed in table 1. The intensity maps are shown in figure 4. For use in the SRO studies, the intensities are given in Laue units (LU); in FePd 1 LU = $39.6 \times 10^{-30} \text{ m}^2$. For comparison, the diffuse intensity profiles obtained from the experimental SRO parameters and the static displacement parameters deduced from the least-squares procedure based on the Borie and Sparks formalism [29] of the neutron diffuse scattering data are also reported. In view of the rather poor statistics, it is remarkable that the main features in position and intensity are reproduced. Namely, the diffuse intensity is mostly concentrated near 100 and equivalent points, i.e. the positions of the superstructure peaks in the long-range ordered $L1_0$ structure. This is not always the case: in the Pt–V and Ni–V systems the SRO diffuse intensity in the disordered phase and the LRO peaks in the ordered phase are differently located [3, 7]. In contrast to the maps deduced from the experimental

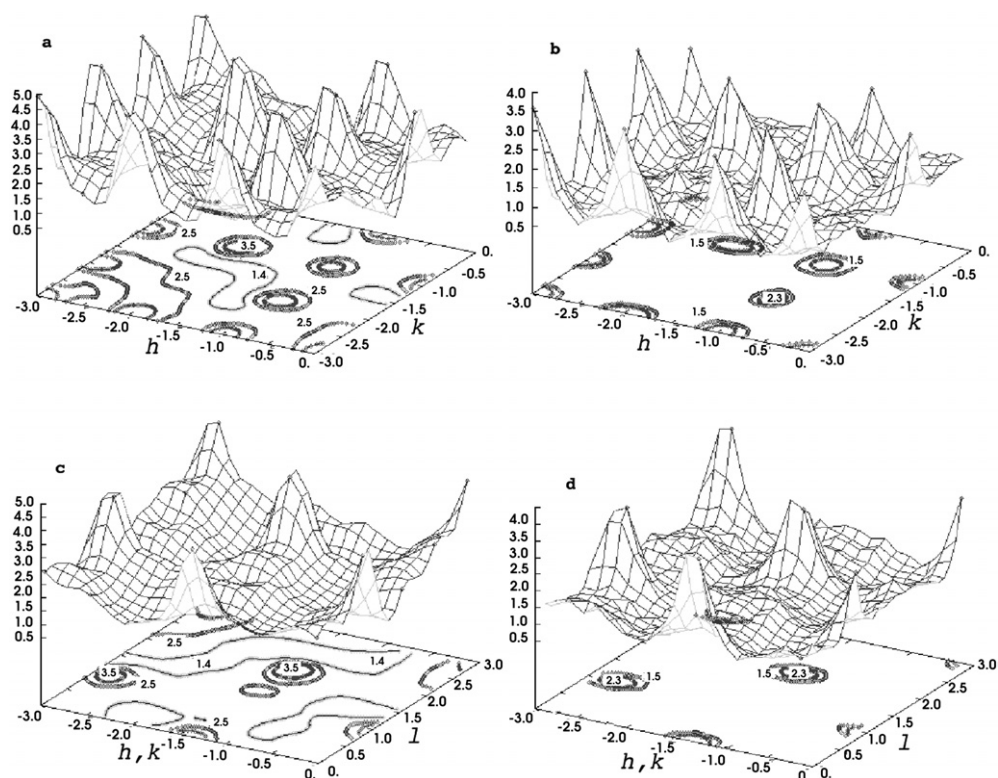


Figure 4. The diffuse scattering intensity (in Laue units) in (100) ((a), (b)) and (110) ((c), (d)) reciprocal planes; as reconstructed from the experimental SRO and the static displacement parameters ((a), (c)) [17] and calculated from the SRO parameters α_n^{cal} listed in table 1 ((b), (d)) (present work).

parameters, we did not take into account any static displacements for the diffuse intensity calculations. Nevertheless, the two profiles agree quite well. This is indicative of a small static displacement in FePd despite the large size difference between Fe and Pd atoms.

The calculated pair interaction energies are summarized in table 1. For comparison, the results of the inverse CVM calculations obtained in FePd using the same set of experimental Warren–Cowley SRO parameters [17] are reported in the same table. One should make clear that the clusters used for the inverse CVM calculations allow only the determination of the first four and the sixth pair interaction energies. Therefore a direct CVM approximation [30] was used to calculate the pair interactions for the fifth neighbour pair and all other pairs from the seventh up the ninth. Despite the many approximations inherent to the inverse CVM calculations, the results of the two methods agree very well. A strong attractive interaction between the second nearest neighbours is evidenced by both inverse CVM and inverse Monte Carlo calculations. The predominance of the second pair interaction has also been recently observed in the Fe–Pt system [31]. A discrepancy is observed for large distances where the inverse Monte Carlo method shows, as expected, that the interactions are vanishing in contrast to the direct CVM results.

Based on the calculated pair interaction energies, Monte Carlo simulation of the order–disorder transition temperature in equiatomic FePd has been performed. The purpose of the calculation was to prove whether the interaction model is appropriate and to examine

the relevance of the pair interaction energies. We have used a model based on the atomic mechanism of order relaxation in dense phases [32]: the vacancy–atom exchange between nearest-neighbour sites. The simulation starts with a perfect $L1_0$ -ordered crystal. One vacancy is introduced at random in the crystal. The vacancy concentration is kept constant during the simulation for all temperatures since we are only interested in the final equilibrium value of the LRO. The equilibrium configuration of the system corresponding to a given temperature was then generated by imposing periodic boundary conditions and letting it relax according to the following algorithm: one nearest neighbour of the vacancy is randomly chosen; the energy balance ΔH of the atom–vacancy exchange is evaluated from an Ising Hamiltonian (equation (1)), considering the final and the initial positions of the jumping atom. We have assumed the relation $v_n^{\text{FeFe}} = v_n^{\text{PdPd}} = -v_n^{\text{FePd}} = V_n$ since it simplifies the algorithm and does not modify the transition temperature [33]. The jump is performed with the Glauber probability.

The variation of the equilibrium LRO parameter as a function of temperature has been followed between 400 and 800 K. The LRO vanishes for temperatures between 700 and 710 K. The uncertainty on the critical temperature due to the standard deviations in the pair interaction energies has been obtained separately by doing simulations taking into account the estimated standard deviation for each V_n . Assuming that the pair interactions are independent and their squared errors can be added, we get a cumulative error of about 160 K; the critical temperature is then equal to $T_c = 705 \pm 160$ K. In view of the many approximations of the Monte Carlo model, the general agreement between the experimental (920 K) and the upper limit of the simulated transition temperatures is quite satisfactory. In fact, experimentally, a 40 K two-phase range is observed at the order–disorder transition in FePd. Besides, the method used here to calculate the LRO parameter, which does not take into account the antiphase domains, only gives an estimate of the transition temperature.

4. Conclusion

Effective pair interaction energies have been deduced in FePd using an inverse Monte Carlo method. The accessible range and the accuracy of the pair interactions have been improved in comparison to the previous inverse and direct CVM calculations. The pair interaction energies have been used to simulate the order–disorder transition temperature in equiatomic FePd. A satisfactory agreement with the experimental value is obtained. The calculated pair interaction energies show the following:

- (i) In contrast to the direct CVM results, the interactions are, as expected, vanishing for large distances, namely, beyond the sixth nearest neighbours.
- (ii) The stability of the $L1_0$ structure of FePd is mainly due to the predominant second pair interaction and the alternating behaviour of V_{lmn} for shells containing like atom (l, m and n all even) and unlike atom pairs (two odds and one even number among l, m and n) in the $L1_0$ ordered structure.
- (iii) The pair interaction range in FePd extends over at least six atomic shells within the error of the experimental data.

In view of those results, a realistic description of the atomic ordering mechanism and order–disorder transformation phenomena in FePd would require the magnitude of interatomic interactions or ordering energies not only for the nearest-neighbour shell, as done in some previous descriptions of the Fe–Pd system [34], but also for higher coordination shells.

References

- [1] Schweika W and Haubold H G 1988 *Phys. Rev. B* **37** 9240
- [2] Pierron-Bohnes V, Kentzinger E, Cadeville M C, Sanchez J M, Caudron R, Solal F and Kozubski R 1995 *Phys. Rev. B* **51** 5760
- [3] Solal F, Caudron R, Ducastelle F, Finel A and Loiseau A 1987 *Phys. Rev. Lett.* **58** 2245
- [4] Schönfeld B, Reinhard L, Kostorz G and Bühner W 1997 *Acta Mater.* **45** 5187
- [5] Capitan M, Lefebvre S, Calvayrac Y, Bessière M and Cénédèse P 1999 *J. Appl. Crystallogr.* **32** 1039
- [6] Kentzinger E, Parasote V, Pierron-Bohnes V, Lami J F and Cadeville M C 2000 *Phys. Rev. B* **61** 14975
- [7] Le Bolloc'h D, Finel A and Caudron R 2000 *Phys. Rev. B* **62** 12082
- [8] Portmann M J, Schönfeld B, Kostorz G and Altorfer F 2001 *Phys. Rev. B* **65** 24110
- [9] Le Bolloc'h D, Robertson J L, Reichert H, Moss S C and Crow M L 2001 *Phys. Rev. B* **63** 35204
- [10] Prem M, Krexner G, Pettinari-Sturmel F and Clement N 2002 *Appl. Phys. A* **74** S1112
- [11] Osaka K and Takama T 2002 *Acta Mater.* **50** 1289
- [12] Cowley J M 1950 *J. Appl. Phys.* **21** 24
- [13] Krivoglaz M A 1966 *Theory of X-ray and Thermal Neutron Scattering by Real Crystals* (New York: Plenum)
- [14] Clapp P C and Moss S C 1966 *Phys. Rev.* **142** 418
- [15] Ducastelle F and Gautier F 1976 *J. Phys. F: Met. Phys.* **6** 2039
- [16] Gratias D and Cénédèse P 1985 *J. Physique Coll.* **46** C9 149
- [17] Mehaddene T, Sanchez J M, Caudron R, Zemirli M and Pierron-Bohnes V 2004 *Eur. Phys. J. B* **41** 207
- [18] Finel A 1994 *Statistics and Dynamics of Alloy Phase Transformation (NATO Advanced Study Institute, Series B: Physics vol 319)* ed P E A Turchi and A Gonis (New York: Plenum) p 495
- [19] Gerold V and Kern J 1987 *Acta Metall.* **35** 393
- [20] Kubachewski O 1982 *Iron Binary Phase Diagrams* (New York: Springer)
- [21] Gehanno V, Marty A, Gilles B and Samson Y 1997 *Phys. Rev. B* **55** 12552
- [22] Kamp P, Marty A, Gilles B, Hoffmann R, Marchesini M, Belakhovsky M, Boeglin C, Dürr H A, Dhesi S S, van der Laan G and Rogalev A 1999 *Phys. Rev. B* **59** 1105
- [23] Tanaka K, Ichitsubo T and Koiwa M 2001 *Mater. Sci. Eng. A* **312** 118
Morioka K and Tanaka K 2001 *PRICM4: Proc. 4th Pacific Rim Int. Conf. on Advanced Materials and Processing* ed S Hanada, Z Zhong, S W Nam and R N Wright (Sendai: The Japan Institute of Metals)
- [24] Bieber A, Gautier F, Treglia G and Ducastelle F 1981 *Solid State Commun.* **39** 149
- [25] Bieber A and Gautier F 1984 *J. Phys. Japan* **53** 2061
- [26] Pierron-Bohnes V, Lefebvre S, Bessière M and Finel A 1990 *Acta Metall. Mater.* **34** 2701
- [27] Pierron-Bohnes V, Cadeville M C, Finel A and Schaerpf O 1991 *J. Physique* **1** 1247
- [28] Proffen T and Neder R B 1997 *J. Appl. Crystallogr.* **30** 171
- [29] Borie B and Sparks J C 1971 *Acta Crystallogr. A* **27** 198
- [30] Kikuchi R 1951 *Phys. Rev.* **81** 988
- [31] Kodera T 2004 *Master Thesis* Graduate School of Engineering, Hokkaido University
Osaka K, Kodera T, Numakura H, Nose Y and Takama T 2004 *134th Mtg of The Japan Institute of Metals (Tokyo)*
- [32] Petry W, Heimig A, Herzig C and Trampenau J 1991 *Defect Diffus. Forum* **75** 211
- [33] Yaldrum K, Pierron-Bohnes V, Cadeville M C and Kahn M A 1999 *J. Mater. Res.* **10** 591
- [34] Chen Y, Atago T and Mohri T 2002 *J. Phys.: Condens. Matter* **14** 1903